Eur. Phys. J. A (2014) **50**: 91
DOI 10.1140/epja/i2014-14091-0

THE EUROPEAN PHYSICAL JOURNAL A

Letter

L-series X-ray yields of kaonic ^{3}He and ^{4}He atoms in gaseous targets

The SIDDHARTA Collaboration

M. Bazzi[1], G. Beer[2], C. Berucci[1,3], A.M. Bragadireanu[1,4], M. Cargnelli[3], C. Curceanu[1], A. d'Uffizi[1], C. Fiorini[5,6], F. Ghio[7], C. Guaraldo[1], R.S. Hayano[8], M. Iliescu[1], T. Ishiwatari[3,a], M. Iwasaki[9], P. Levi Sandri[1], J. Marton[3], S. Okada[9], D. Pietreanu[1,4], T. Ponta[4], R. Quaglia[5,6], A. Romero Vidal[11], E. Sbardella[1], A. Scordo[1], H. Shi[3], D.L. Sirghi[1,4], F. Sirghi[1,4], H. Tatsuno[1,b], O. Vazquez Doce[1,10], B. Wünschek[3], E. Widmann[3], and J. Zmeskal[3]

[1] INFN, Laboratori Nazionali di Frascati, C.P. 13, Via E. Fermi 40, I-00044 Frascati (Roma), Italy
[2] Department of Physics and Astronomy, University of Victoria, P.O. Box 1700 STN CNC, Victoria BC V8W 2Y2, Canada
[3] Stefan-Meyer-Institut für subatomare Physik, Boltzmanngasse 3, 1090 Wien, Austria
[4] IFIN-HH, Institutul National pentru Fizica si Inginerie Nucleara Horia Hulubei, Reactorului 30, Magurele, Romania
[5] Politecnico di Milano, Dipartimento di Elettronica, Informazione e Bioingegneria, Milano, Italy
[6] INFN, Sezione di Milano, Milano, Italy
[7] INFN, Sezione di Roma I and Instituto Superiore di Sanità, I-00161 Roma, Italy
[8] University of Tokyo, 7-3-1, Hongo, Bunkyo-ku, Tokyo, Japan
[9] RIKEN, Institute of Physical and Chemical Research, 2-1 Hirosawa, Wako, Saitama 351-0198, Japan
[10] Excellence Cluster Universe, Technische Universität München, Boltzmannstraße 2, D-85748 Garching, Germany
[11] Universidade de Santiago de Compostela, Casas Reais 8, 15782 Santiago de Compostela, Spain

Received: 20 February 2014 / Revised: 25 April 2014
Published online: 28 May 2014

Communicated by P. Salabura

Abstract. The SIDDHARTA experiment measured X-rays from kaonic helium atoms using, for the first time, gaseous ^{3}He and ^{4}He targets. Clear patterns of the L-series X-rays of kaonic ^{3}He and ^{4}He atoms were observed. By using accurate Monte Carlo simulations, the absolute yields of these X-ray transitions were determined to be $Y(3d \to 2p) = 25.0^{+6.7}_{-5.8}\%$ for ^{3}He (0.96 g/l), $Y(3d \to 2p) = 23.1^{+6.0}_{-4.2}\%$ for ^{4}He (1.65 g/l), and $Y(3d \to 2p) = 17.2^{+2.6}_{-9.5}\%$ for ^{4}He (2.15 g/l). In addition, the yields $Y(nd \to 2p)$, with $n > 3$ were also determined. The measured yields provide valuable information for understanding the cascade processes of kaonic helium atoms as a function of the target density.

1 Introduction

Measurements of kaonic helium $2p$ X-rays were performed in the 70's and 80's using liquid ^{4}He targets [1–3]. The absolute X-ray yields were about half the values predicted by cascade models [3,4]. The smaller absolute X-ray yields indicate a large absorption from the higher principal number n states due to the strong Stark mixing and to external Auger transitions at the liquid density.

The process of Stark mixing in exotic helium atoms is different from that of hydrogen. When an exotic particle X^- is captured by a helium atom in highly excited states ($n \sim 30$ for kaonic helium), it immediately de-excites by the internal Auger process, emitting the remaining electron, and forms the hydrogen-like positive ion $(X^-, \alpha)^+$. The $(X^-, \alpha)^+$ is Coulomb repelled by nearby helium atoms, thus the Day-Snow-Sucher type of Stark mixing [5] does not occur. However, the $(X^-, \alpha)^+$ ion induces a molecular electric field by polarizing neighboring helium atoms while in collision, and then the so-called molecular Stark mixing occurs [6]. Moreover, the $(X^-, \alpha)^+$ ion can form a molecular ion state with another neutral helium atom $[^4\text{He} - (X^-, \alpha)]^+$ in three-body collision processes —so-called molecular ion formation (MIF) [7]. The molecular ion subsequently de-excites by the external Auger transitions which are competing with the radiative transitions.

The cascade calculations of exotic helium atoms have been developed by taking into account the above molecular effects. Baker *et al.* [8] calculated the X-ray yields of $\bar{p}^4$He by adjusting the free parameters of Stark mixing and external Auger effects. Their results were in good agreement with experimental data at various gas, but not liquid densities, because the MIF was not included. Landua and Klempt [9] independently developed the Monte Carlo cal-

[a] e-mail: tomoichi.ishiwatari@assoc.oeaw.ac.at
[b] e-mail: tatsuno@lnf.infn.it

culation method without using any free parameters for the molecular effects, and reproduced the μ^{-4}He and π^{-4}He X-ray yields at both gas and liquid densities. Later they refined their model and successfully described the density dependent X-ray yields of μ^{-4}He [10], $\bar{p}^4$He and $\bar{p}^3$He [11].

For kaonic helium, Koike and Akaishi developed a realistic calculation model of the Stark mixing by using the impact-parameter method [12]. They included the MIF effects and reproduced the $\bar{p}^4$He and K^{-4}He X-ray yields at liquid density by adjusting the strength of MIF and the molecular Stark mixing rate. Although this calculation solved the disagreement among the absolute intensities of K^{-4}He X-rays, the free parameters remained to be determined.

An experimental measurement with a gaseous helium target makes it possible to study the density dependent Stark mixing effect by removing the influence of MIF, because the MIF predominantly occurs at the liquid density.

The SIDDHARTA experiment [13–15] successfully measured the K^{-3}He and K^{-4}He X-ray transitions to the $2p$ states using gaseous targets for the first time. The absolute yields in gas were determined by using the Monte Carlo simulations, and are reported in this letter.

2 The SIDDHARTA experiment

Kaonic atom X-rays from gaseous targets were measured by the SIDDHARTA experiment at the DAΦNE collider at LNF-INFN (Italy). K^+K^- pairs produced by ϕ decay were emitted from the interaction point. The K^+K^- pairs were detected by a kaon detector consisting of two plastic scintillators placed above and below the beam pipe. The timing signals of the K^+K^- pairs were recorded using clock signals with a frequency generated by DAΦNE.

Because of the finite crossing angle of the electron and positron beams, the momentum of the emitted kaons had an angular dependence, which was compensated using a stepped degrader made of Mylar foils with thicknesses ranging from 100 to 800 μm.

The charged kaons entered the target cell after passing through the scintillator and degrader. The cylindrical target cell was made of Kapton polyimide ($C_{22}H_{10}N_2O_5$) foils with a thickness of 75 μm and a density of 1.42 g/cm^3. The bottom of the target cell, through which the charged kaons entered, was also made of Kapton.

The X-rays were measured by silicon drift detectors (SDDs) [16], which surrounded the target. Each SDD had an effective area of 1 cm^2 with a 450 μm thickness. There were 144 SDDs in total. Among them, 94 SDDs with best performance were selected in the analysis. The SDDs were cooled to a temperature of 170 K to obtain an excellent energy resolution of about 150 eV (FWHM) for 6 keV X-rays, which is close to the resolution in noise-free conditions.

The data on the kaonic atom X-rays were accumulated in 2009. In the experiment, we used four target gases: hydrogen (1.30 g/l) [17,18], deuterium (2.50 g/l) [19], ^{3}He (0.96 g/l) [14,15] and ^{4}He (1.65 g/l and 2.15 g/l) [13,15]. They were cooled to 23 K. The charged kaons stopped mainly in the target gas and partially in the Kapton windows.

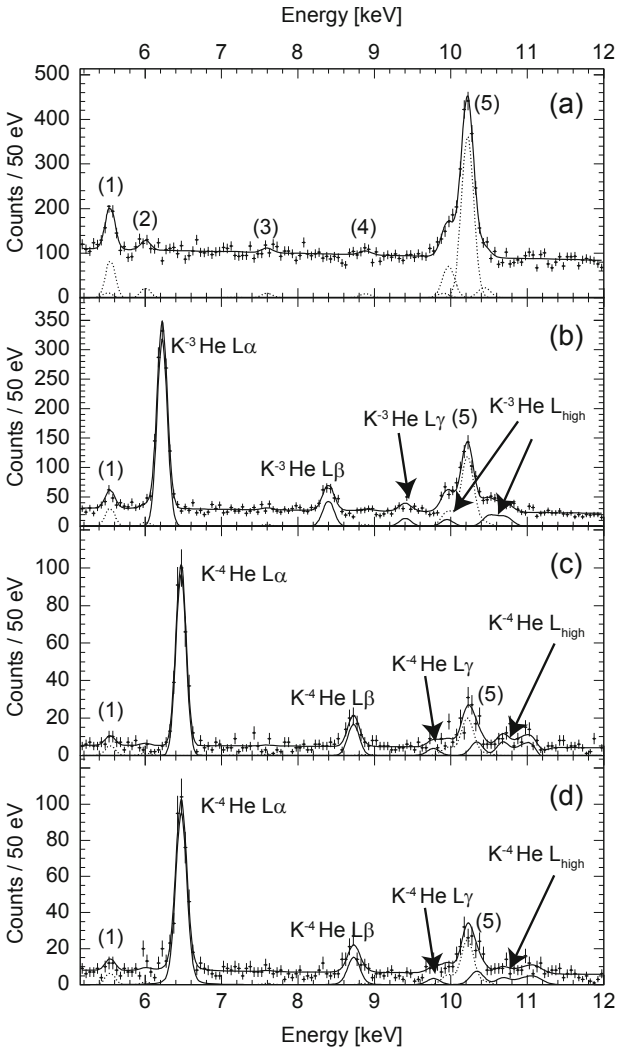

Fig. 1. Energy spectra taken with (a) deuterium (2.50 g/l), (b) ^{3}He (0.96 g/l), (c) ^{4}He (1.65 g/l), and (d) ^{4}He (2.15 g/l) targets. (1) Kaonic carbon (K^-C) $8 \to 6$ and $6 \to 5$, (2) kaonic oxygen (K^-O) $7 \to 6$, (3) kaonic nitrogen (K^-N) $6 \to 5$, (4) K^-N $7 \to 5$, (5) K^-O $8 \to 6$ and $6 \to 5$, K^-C $5 \to 4$, and kaonic aluminum (K^-Al) $8 \to 7$ transitions. The fit lines in the energy spectra are also shown. The dotted lines show the fit functions of the X-ray transitions produced in Kapton after the background subtraction. The solid lines show the fit functions of the kaonic helium X-ray lines after the background subtraction. The positions of the kaonic helium X-ray lines in (b)–(d) are indicated by arrows.

3 Data analysis

The data from the SDDs and the kaon detector were analyzed to extract energy spectra of kaonic atom X-rays with a good signal-to-background ratio. The analysis method described in [20] was applied here. Figure 1 shows energy spectra taken with a target of (a) deuterium (2.50 g/l), (b) ^{3}He (0.96 g/l), (c) ^{4}He (1.65 g/l), and (d) ^{4}He (2.15 g/l). In the figures, X-ray peaks of kaonic atoms were observed as well as a continous flat background originating from the beam losses and ϕ-decay particles.

The X-ray peaks observed in fig. 1(a) were identified with X-ray transitions produced in Kapton [20]. A detailed description of the identification of the observed peaks is given in [20]. The largest peak, seen around 10.5 keV, is the kaonic carbon (K^-C) $5 \to 4$ transition. The identification of other peaks is shown in the caption of the figure. The dotted lines show the fit functions of the X-ray transitions produced in Kapton after the background subtractions. Because these peaks were produced in the target window material made of Kapton, they can be observed in the different gaseous targets with the same relative intensities. It is to be noted that signals from kaonic deuterium were negligible in this fit, where the upper limit of the kaonic deuterium signals was described in [19].

Figure 1(b) shows the energy spectrum taken with a target of ^{3}He gas (0.96 g/l). The peak at 6.2 keV was identified as the kaonic ^{3}He $L\alpha$ ($3d \to 2p$) line. Other kaonic ^{3}He lines are shown in the figure as well. The solid lines show the fit functions of the kaonic helium X-ray lines after the background subtraction. The positions of the kaonic helium X-ray lines were indicated by arrows. Here, the sum of the $nd \to 2p$ transitions with ($n \geq 6$) was indicated as $L_{\rm high}$.

In the fit of the energy spectrum, the contamination by the X-ray lines from Kapton was evaluated using the value determined from the energy spectrum taken with deuterium. In the fit of the spectrum, the relative ratios of the X-ray lines from Kapton to the K^-C $5 \to 4$ line were fixed to the values obtained with the deuterium gas, whereas the intensity of the K^-C $5 \to 4$ line was taken as a free parameter.

Figures 1(c) and (d) show the energy spectra taken with ^{4}He gas with a density of 1.65 g/l and 2.15 g/l, respectively. The peak at 6.4 keV was identified as the kaonic ^{4}He $L\alpha$ ($3d \to 2p$) line, while the other kaonic ^{4}He lines were also shown in the figure. The intensities of the kaonic ^{4}He X-ray lines were extracted using the same method as used on the kaonic ^{3}He data.

The numbers of X-rays observed in the spectra are summarized in table 1, where the errors include the uncertainties from the Kapton contamination. The numbers of X-rays were determined by the fit using a Voigt function. The numbers of K^+K^- events detected by the kaon detector ($N_{\rm trig}^{\rm EXP}$) are also shown in the table.

4 Monte Carlo simulations

Monte Carlo simulations are needed to evaluate the number of kaons stopping in the gas targets, needed to extract the absolute X-ray yields. In addition, X-ray attenuation in the target gases and target windows, as well as X-ray detection efficiencies of the SDDs were extracted from the simulations.

The Monte Carlo simulation code was based on the GEANT4 toolkit, where all the materials and geometries used in the experiment were included. The detailed description of the Monte Carlo simulation is given in [20]. Here we briefly summarize the method.

Table 1. The number ($N_{\rm X}^{\rm EXP}$) of kaonic helium X-rays measured in the experiment and detection efficiencies ($\epsilon^{\rm MC}$) of the X-rays determined by Monte Carlo simulations. The number ($N_{\rm trig}^{\rm EXP}$) of K^+K^- events measured in the experiment is also shown.

Target ($N_{\rm trig}^{\rm EXP} \cdot 10^6$)	Transition	$N_{\rm X}^{\rm EXP}$	$\epsilon^{\rm MC}$ 10^{-4}
^{3}He	$L\alpha$	1095 ± 42	$23.87^{+5.48}_{-6.32}$
0.96 g/l	$L\beta$	174 ± 19	$26.32^{+4.40}_{-8.67}$
(1.832)	$L\gamma$	63 ± 15	$26.08^{+5.57}_{-7.81}$
	$L_{\rm high}$	250^{+74}_{-73}	$26.10^{+7.06}_{-7.67}$
^{4}He	$L\alpha$	326 ± 19	$47.04^{+25.80}_{-6.48}$
2.15 g/l	$L\beta$	62 ± 10	$50.48^{+24.71}_{-7.14}$
(0.403)	$L\gamma$	14 ± 7	$50.91^{+23.44}_{-7.61}$
	$L_{\rm high}$	85 ± 18	$50.81^{+22.99}_{-7.83}$
^{4}He	$L\alpha$	382 ± 25	$35.24^{+5.99}_{-8.92}$
1.65 g/l	$L\beta$	73 ± 12	$36.87^{+7.26}_{-6.96}$
(0.470)	$L\gamma$	22 ± 9	$36.11^{+9.34}_{-5.87}$
	$L_{\rm high}$	121 ± 21	$37.06^{+7.96}_{-8.79}$

The simulation starts with the production of the charged kaon pairs (K^+K^-) at the interaction point. In the production of K^+K^- pairs, the ϕ-boost effect, the size of the interaction region and the polar angular distribution of the K^+K^- pairs were included. The number of kaon triggers was counted as the number of K^+K^- events recorded in the kaon detector.

The modeling of X-ray generation from kaonic atoms was done in the at-rest process of the GEANT4 code. The kaonic atom X-rays were generated at the position where the K^- stopped, and were isotropically emitted with a 100% yield for each transition and each kaonic atom. The energies of the X-rays were fixed to the values measured experimentally. The number and position of the SDDs used in the simulation are the same as those used to obtain the measured spectra.

The efficiency ($\epsilon^{\rm MC}$) in the simulation is defined as the number of X-rays detected by the SDDs divided by the number of kaon triggers.

$$\epsilon^{\rm MC} = \frac{N_{\rm X}^{\rm MC}}{N_{\rm trig}^{\rm MC}}. \quad (1)$$

The predicted efficiencies are shown in table 1, where the errors include the uncertainty of the simulation.

5 Results and discussion

The absolute X-ray yield is defined as the X-ray intensity per stopped kaon. However, the number of kaons stopping in the targets was not measured experimentally. Instead, in our method, the number of stopping kaons was evaluated by the Monte Carlo simulations. Thus, comparing the

Table 2. Absolute X-ray yields of $K^-{}^3$He and $K^-{}^4$He measured in gas targets. The yields are shown in percentages per stopped K^-. The experimental results for liquid ^{4}He, refs. [1,3], are also shown in the last columns. The value of $L_{\rm high}$ in the liquid density data [3] includes the contribution of $L\delta$ only.

Transition	^{3}He (0.96 g/l)	^{4}He (1.65 g/l)	^{4}He (2.15 g/l)	^{4}He (Liquid) [1]	^{4}He (Liquid) [3]
$L\alpha$	$25.0^{+6.7}_{-5.8}$	$23.1^{+6.0}_{-4.2}$	$17.2^{+2.6}_{-9.5}$	9.2 ± 2.4	8.9 ± 4.5
$L\beta$	$3.6^{+1.3}_{-0.7}$	4.2 ± 1.1	$3.1^{+0.6}_{-1.6}$	5.2 ± 1.3	2.3 ± 1.2
$L\gamma$	$1.3^{+0.5}_{-0.4}$	1.3 ± 0.6	$0.7^{+0.3}_{-0.5}$	2.4 ± 0.7	1.6 ± 0.8
$L_{\rm high}$	5.2 ± 2.1	$6.9^{+2.0}_{-1.9}$	$4.1^{+1.1}_{-2.1}$	–	$0.4 \pm 0.3^*$

efficiencies determined by the measurements and simulations, the X-ray yields of kaonic helium can be obtained. In performing the comparison, the normalization was done using the number of K^+K^- events detected by the kaon detector. The absolute X-ray yield (Y) per stopped K^- was then calculated as

$$Y = \frac{\epsilon^{\rm EXP}}{\epsilon^{\rm MC}} = \frac{N_{\rm X}^{\rm EXP}/N_{\rm trig}^{\rm EXP}}{\epsilon^{\rm MC}}. \quad (2)$$

The results of the absolute X-ray yields of $K^-{}^3$He and $K^-{}^4$He are summarized in table 2. The previous results of $K^-{}^4$He yields in liquid, refs. [1,3], are also shown. The yields of the $L\alpha$ lines in gas are about 2.0–2.5 times higher than those in liquid, while the yields of the $L\beta$ and $L\gamma$ lines are consistent. The intensities of the $L_{\rm high}$ lines in gas are obviously higher than those in liquid. These yield differences are related to the density dependence of the cascade processes, such as the molecular Stark effect and MIF.

6 Conclusions

The SIDDHARTA experiment measured the patterns of the X-ray transitions to the $2p$ states for kaonic ^{3}He and ^{4}He atoms using gaseous targets. The absolute X-ray yields of L-series lines in gas were determined for the first time. The observed high yields of $L\alpha$ and $L_{\rm high}$ lines indicate weaker molecular Stark mixing and a small influence of MIF at gas densities. Further improvements of cascade calculations based on the data given in this Letter are eagerly awaited to better understand the cascade processes of kaonic helium atoms.

We thank C. Capoccia, G. Corradi, B. Dulach, and D. Tagnani from LNF-INFN; and H. Schneider, L. Stohwasser, and D. Stückler from Stefan Meyer Institute, for their fundamental contribution in designing and building the SIDDHARTA setup. We thank as well the DAΦNE staff for the excellent working conditions and permanent support. Discussions with T. Koike are gratefully acknowledged. Part of this work was supported by HadronPhysics I3 FP6 European Community program, Contract No. RII3-CT-2004-506078; the European Community-Research Infrastructure Integrating Activity "Study of Strongly Interacting Matter" (HadronPhysics 2, Grant Agreement No. 227431), and HadronPhysics 3 (HP3), Contract No. 283286 under the Seventh Framework Programme of EU; Austrian Federal Ministry of Science and Research BMBWK 650962/0001 VI/2/2009; Romanian National Authority for Scientific Research, Contract No. 2-CeX 06-11-11/2006; the Grant-in-Aid for Specially Promoted Research (20002003), MEXT, Japan; and the Austrian Science Fund (FWF): [P24756-N20].

References

1. C.E. Wiegand, R. Pehl, Phys. Rev. Lett. **27**, 1410 (1971).
2. C.J. Batty *et al.*, Nucl. Phys. A **326**, 455 (1979).
3. S. Baird *et al.*, Nucl. Phys. A **392**, 297 (1983).
4. S. Berezin *et al.*, Phys. Lett. B **30**, 1969 (27).
5. T.B. Day, G.A. Snow, J. Sucher, Phys. Rev. Lett. **3**, 61 (1959).
6. T.B. Day, G.A. Snow, Phys. Rev. Lett. **5**, 112 (1960).
7. J.E. Russell, Phys. Rev. A **18**, 521 (1978).
8. C.A. Baker *et al.*, Nucl. Phys. A **494**, 507 (1989).
9. R. Landua, E. Klempt, Phys. Rev. Lett. **48**, 1722 (1982).
10. G. Reifenröther, E. Klempt, R. Landua, Phys. Lett. B **191**, 15 (1987).
11. G. Reifenröther, E. Klempt, R. Landua, Phys. Lett. B **203**, 9 (1988).
12. T. Koike, Y. Akaishi, Nucl. Phys. A **639**, 521c (1998).
13. SIDDHARTA Collaboration, Phys. Lett. B **681**, 310 (2009).
14. SIDDHARTA Collaboration, Phys. Lett. B **697**, 199 (2011).
15. SIDDHARTA Collaboration, Phys. Lett. B **714**, 40 (2012).
16. SIDDHARTA Collaboration, Nucl. Instrum. Methods A **581**, 326 (2007).
17. SIDDHARTA Collaboration, Phys. Lett. B **704**, 113 (2011).
18. SIDDHARTA Collaboration, Nucl. Phys. A **881**, 88 (2012).
19. M. Bazzi *et al.*, Nucl. Phys. A **907**, 69 (2013).
20. SIDDHARTA Collaboration, Nucl. Phys. A **916**, 30 (2013).